



ON THE STEADY STATE AND DYNAMIC CHARACTERISTICS OF OIL JOURNAL BEARINGS WITH MULTIPLE AXIAL GROOVES

L. Roy¹ and P. L. Choudhury¹

¹Department of Mechanical Engineering, National Institute of Technology, Silchar, India

E-mail: lintu_roy@yahoo.com

ABSTRACT

The steady state and dynamic characteristics including whirl instability of journal bearings with three axial groove, one located at the top and another two 90 degrees clockwise and anticlockwise from the top, from which oil is supplied from one end of the bearing; a linear pressure drop is assumed in the groove and the steady state and dynamic characteristics are obtained theoretically. The Reynolds equation is solved numerically by finite difference method satisfying the appropriate boundary conditions. The dynamic behaviors in terms of stiffness and damping coefficients of fluid film and stability are found using a first-order perturbation method. It has been shown that both load capacity and stability improve for smaller groove angle is stability improved at higher eccentricity ratio.

Keywords: axial groove, journal bearings, stability, steady state characteristics, linear pressure drop.

NOTATION

C	radial clearance (m)
D	diameter of the journal (m)
$D_{rr}, D_{\phi\phi}, D_{r\phi}, D_{\phi r}$	damping coefficients (N s /m)
$\bar{D}_{rr}, \bar{D}_{\phi\phi}, \bar{D}_{r\phi}, \bar{D}_{\phi r}$	non-dimensional damping coefficients, ($\bar{D}_{ij} = D_{ij}C\omega / (LDp_s)$)
e	eccentricity (m)
h, \bar{h}	local film thickness (m), $\bar{h} = h / C$
$K_{rr}, K_{\phi\phi}, K_{r\phi}, K_{\phi r}$	stiffness coefficients (N/m)
$\bar{K}_{rr}, \bar{K}_{\phi\phi}, \bar{K}_{r\phi}, \bar{K}_{\phi r}$	non-dimensional stiffness coefficients, ($\bar{K}_{ij} = K_{ij}C / (LDp_s)$)
L	length of the bearing (m)
M, \bar{M}	rotor mass per bearing (kg), $\bar{M} = MC\omega^2 / LDp_s$
p, \bar{p}	film pressure (Pa), $\bar{p} = p / p_s$
p_s	supply pressure (Pa)
η	coefficient of absolute viscosity of the lubricant (Pa-s)
Q, \bar{Q}	end flow of oil (m ³ /s), $\bar{Q} = 2Q\eta L / (C^3 Dp_s)$
R	journal radius (m)
t	time (s)
W, \bar{W}	load capacity (N), $\bar{W} = W / (LDp_s)$
α	groove angle (deg)
ε	eccentricity ratio, $\varepsilon = e / C$
θ, \bar{z}	non-dimensional coordinates, $\theta = x / R, \bar{z} = z / (L / 2)$
λ	whirl ratio = ω_p / ω
Λ	bearing number, $6\eta\omega / [p_s(C / R)^2]$
$\mu, \bar{\mu}$	coefficient of friction, $\bar{\mu} = \mu(R / C)$
τ	non-dimensional time, $\tau = \omega_p t$
ϕ	attitude angle (rad)
ψ	assumed attitude angle (rad)
ω	journal rotational speed (rad/s)



ω_p	frequency of journal vibration (rad/s)
$()_0$	steady state value

1. INTRODUCTION

In the classical work, Sommerfeld [1] found analytical solution of infinitely long oil journal bearings with a single oil hole located at the unloaded region. Orvik [2], using a narrow bearing approximation, provided a steady state solution of full oil journal bearings. Later Christopherson [3] and Raimondi and Boyd [4] gave numerical solutions of finite oil journal bearings. The investigation of cavitation in the lubricating film was initiated by Coles and Hughes [5]. Akers and Flack [6] have provided linear transient method. Allaire and Flack [6] have provided a detailed discussion on the design and application of various oil journal bearing configurations. The above mentioned work relates to the plain cylindrical oil journal bearings. In recent years, Yoshimoto *et al.*, [8] considered axial load capacity and stability of water lubricated hydrostatic conical bearings with spiral grooves. Analysis of water lubricated journal bearings with multiple axial grooves is carried out by Majumder, Pai and Hargreaves [9]. The bearing configuration studied here in the present case is a three-grooved journal bearing. The lubricant is fed from one end through the three axial grooves (groove angle being 36° and 18°). The lubricant film is generated in the land region. The flow in this region will be both circumferential and axial. The lubricant flows out from the bearing end axially. The pressure generated due to wedge action in the clearance space supports the load without metal-to-metal contact. In the normal situation the pressures drop in the groove likely to be linear from the entrance to the exit end. The governing equation is the Reynolds Equation in two dimensions. This equation is solved for pressure numerically satisfying the boundary condition. In addition Swift-Stieber boundary conditions are adopted if cavitations occur in the divergent portion. The pressure distribution in the clearance space gives the steady state characteristics in terms of load carrying capacity, attitude angle, volume flow rate and co-efficient of fluid friction. With these data a preliminary design of the bearing can be made. As the fluid film bearing are prone to whirl instability to some extent, a further study is undertaken to obtain the dynamic characteristics in terms of stiffness and damping of fluid film and stability of the rotor bearing system. The time dependant Reynolds equation in two dimensions is to be solved for this purpose. A first order perturbation method is used to find the dynamic pressures in the clearance space. The stiffness and damping dynamic pressure in the clearance space. The stiffness and damping coefficients are then used in the equation of motion of a rigid rotor for estimating the mass parameter, a measure of stability. When these bearing are used in high speed machinery, the stability is an important consideration.

2. THEORY

The governing equation is the Reynolds equation in two dimensions for an incompressible fluid (Figure-1). It can be written in dimensionless form as:

$$\frac{\partial}{\partial \theta} (h^{-3} \frac{\partial \bar{p}}{\partial \theta}) + (D/L)^2 h^{-3} \frac{\partial^2 \bar{p}}{\partial z^2} = \Lambda \frac{\partial \bar{h}}{\partial \theta} + 2\Lambda \lambda \frac{\partial \bar{h}}{\partial \tau} \quad (1)$$

2.1. Steady state characteristics

Under steady state condition equation (1) can be reduced to

$$h_0^{-3} \frac{\partial^2 \bar{p}_0}{\partial \theta^2} + 3h_0^{-2} \frac{\partial \bar{h}_0}{\partial \theta} \frac{\partial \bar{p}_0}{\partial \theta} + (D/L)^2 h_0^{-3} \frac{\partial^2 \bar{p}_0}{\partial z^2} - \Lambda \frac{\partial \bar{h}_0}{\partial \theta} = 0 \quad (2)$$

For axially grooved journal bearings, the boundary conditions are

$$\bar{p}_0 = 1 \text{ at one end of the groove where the supply of oil starts, } \bar{p}_0 = 0 \text{ at the bearing ends and the pressure is set equal to 0 when the pressure falls below zero.} \quad (3)$$

In a conventional cylindrical bearing the coordinate θ in the circumferential direction is taken from the position of maximum film thickness. Here in the grooved bearing this position needs to be found beforehand. This is done by assuming an arbitrary value of attitude angle ψ and the coordinate Θ is measured from the vertical position, as shown in Fig.1. Using this ψ the film thickness equation can be written as $\bar{h}_0 = 1 + \varepsilon_0 \cos(\Theta - \psi)$. The equation (2) is solved numerically by finite difference method using the boundary conditions of the equation (3). The load components along the line of centres and its perpendicular direction are found from

$$\bar{W}_r (= \frac{W_r}{LDp_s}) = -\frac{1}{2} \int_0^{2\pi} \int_0^1 \bar{p}_0 \cos(\Theta - \psi) d\theta d\bar{z} \quad (4a)$$

$$\bar{W}_t (= \frac{W_t}{LDp_s}) = \frac{1}{2} \int_0^{2\pi} \int_0^1 \bar{p}_0 \sin(\Theta - \psi) d\theta d\bar{z} \quad (4b)$$

The load capacity and attitude angle are given by

$$\bar{W} = [\bar{W}_r^2 + \bar{W}_t^2]^{1/2} \quad (5)$$

$$\phi_0 = \tan^{-1} \left(\frac{\bar{W}_t}{\bar{W}_r} \right) \quad (6)$$

The pressure distribution for $L/D=1$, $\Lambda=10.0$ is shown in Figure-2. The attitude angle calculated from equation (6) is compared with the assumed value of attitude angle (ψ). The value of ψ is modified with a



small increment of ψ and the Reynolds equation is solved using the modified value until ψ is equal to ϕ_0 . The volume rate of flow and the coefficient of friction are calculated from the pressure distribution. The flow rate in the dimensionless form can be written as

$$\bar{Q} (= \frac{2Q\eta L}{C^3 p_s D}) = -\frac{1}{3} \int_0^{2\pi} \bar{h}_0^3 \frac{\partial \bar{p}_0}{\partial \bar{z}} \Big|_{\bar{z}=1} d\theta \quad (7)$$

Friction variable is given by $\bar{\mu} = (\frac{R}{C})\mu = \frac{\bar{F}}{\bar{W}}$

Where

$$\bar{F} (= \frac{F}{2LCp_s}) = \int_0^1 \int_0^{2\pi} \left(\frac{1}{4} \bar{h}_0 \frac{\partial \bar{p}_0}{\partial \theta} + \frac{\Lambda}{12} \frac{1}{\bar{h}_0} \right) d\theta d\bar{z}$$

Since no cavitation was observed, the integrations were carried out from 0 to 2π .

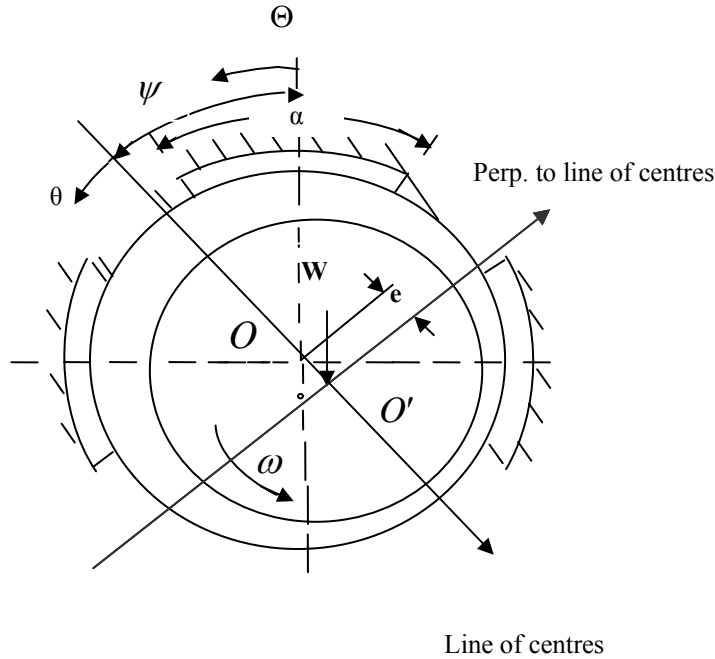


Figure-1. Multiple axial grooved journal bearing with co-ordinate system.

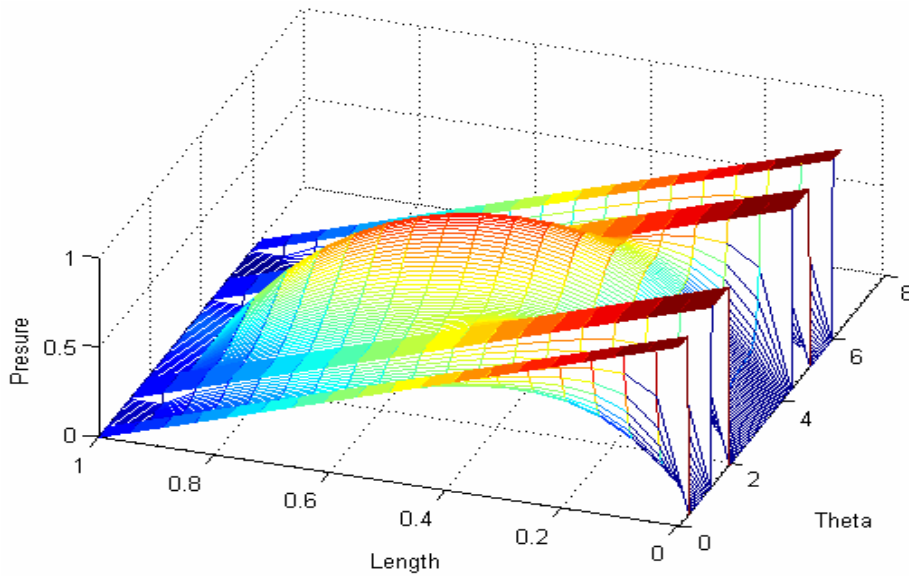


Figure-2. Pressure distribution for $L/D = 1$, $\Lambda = 10.0$ and groove angle 36° .



2.2. Dynamic characteristics

The Reynolds equation under dynamic condition is the equation (1). The pressure and film thickness can be expressed for small amplitude of vibration as:

$$\bar{p} = \bar{p}_0 + \varepsilon_1 e^{i\tau} \bar{p}_1 + \varepsilon_0 \phi_1 e^{i\tau} \bar{p}_2 \quad (8)$$

$$\bar{h} = \bar{h}_0 + \varepsilon_1 e^{i\tau} \cos \theta + \varepsilon_0 \phi_1 e^{i\tau} \sin \theta \quad (9)$$

Substitution of equations (8) and (9) into the equation (1) and retaining the first linear terms, gives the

$$\bar{M} = \frac{1}{\lambda^2 (\bar{D}_{\phi\phi} + \bar{D}_{rr})} \left[(\bar{K}_{rr} \bar{D}_{\phi\phi} + \bar{D}_{rr} \bar{K}_{\phi\phi}) - (\bar{K}_{\phi r} \bar{D}_{r\phi} + \bar{D}_{\phi r} \bar{K}_{r\phi}) - \frac{\bar{W}}{\varepsilon_0} (\bar{D}_{\phi r} \bar{W} \sin \phi_0 - \bar{D}_{rr} \bar{W} \cos \phi_0) \right] \quad (10)$$

$$\begin{aligned} \bar{M}^2 \lambda^4 - \lambda^2 \left[\bar{M} \left(\frac{\bar{W}_0 \cos \phi_0}{\varepsilon_0} + \bar{K}_{\phi\phi} + \bar{K}_{rr} \right) + (\bar{D}_{rr} \bar{D}_{\phi\phi} - \bar{D}_{\phi r} \bar{D}_{r\phi}) \right] \\ + (\bar{K}_{rr} \bar{K}_{\phi\phi} - \bar{K}_{\phi r} \bar{K}_{r\phi}) + \frac{\bar{W}_0}{\varepsilon_0} (\bar{K}_{rr} \cos \phi_0 - \bar{K}_{\phi r} \sin \phi_0) = 0 \end{aligned} \quad (11)$$

Equations (10) and (11) are linear algebraic equations in \bar{M} and λ and solution of these will give \bar{M} and λ . The speed of the journal calculated from this value of \bar{M} is the threshold speed, above which the bearing system will be unstable.

3. RESULTS AND DISCUSSION

3.1. Analysis of results for the bearing feeding from the end of the groove

When the bearing operates at a small speed, the hydrodynamic effect is not predominant. Thus it is difficult to run the bearing at low speeds. Therefore, there

three differential equations in \bar{p}_0, \bar{p}_1 and \bar{p}_2 . The equations for \bar{p}_1 and \bar{p}_2 are solved satisfying the modified boundary conditions of equation (3) and known values of \bar{p}_0 .

Following an approach given by Majumdar, Brewster and Khonsari [8], stiffness and damping coefficients are found and used in the equations of motion to obtain the following equations,

is a speed below which the bearing cannot be operated. In this present analysis, it has been found that the limiting value of non-dimensional speed parameter is $\Lambda = 5$. To be on the safe side, we have considered the speed parameter Λ is above 10.

Before discussing on the results, the flow rates are compared with the approximate formula (Table-1) given by Martin and Lee [7]. The flow rate calculated from the present method of solution gives higher value because the flow is due to feed pressure and hydrodynamic pressure.

Table-1. Comparison of non dimensional flow rate with reference [7] for 36° and 18° groove angle, L/D = 1.0, $\Lambda = 10.0$.

L/D ratio	ε_0	\bar{Q}	\bar{Q} (Martin and Lee) [7]
1	0.2	3.1926 (3.1925)	1.2813 (1.1546)
	0.4	4.2619 (4.2610)	1.8175 (1.6108)
	0.6	5.769 (5.7687)	2.7000 (2.4417)
	0.8	7.5015 (7.5006)	4.3750 (4.0958)

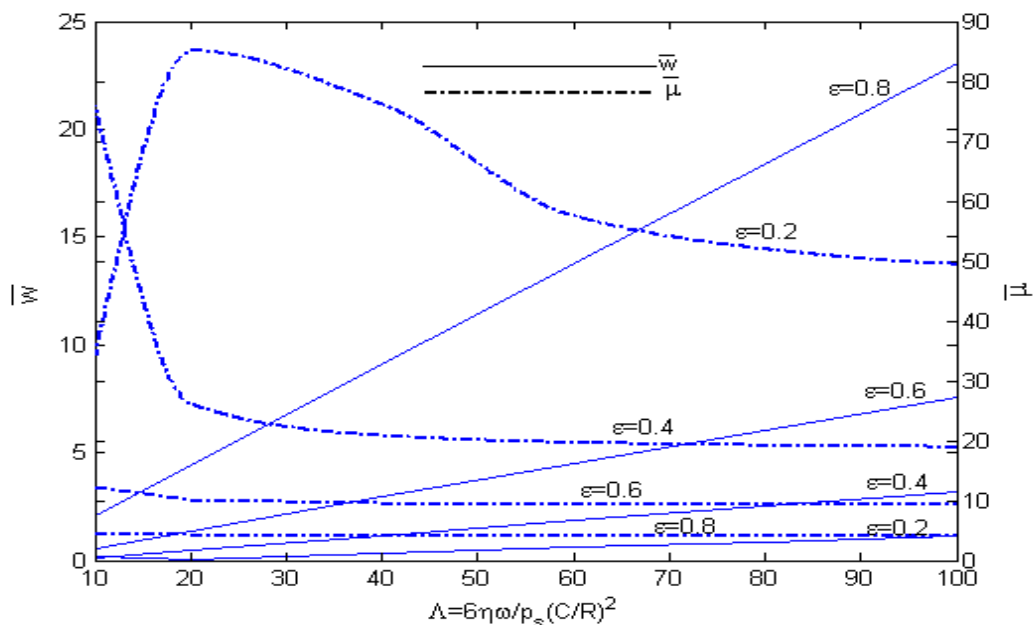
* Terms in the bracket indicate the corresponding values for 18° grooved angle bearing.

**Table- 2.** Comparison of 36° and 18° groove angle bearing having L/D = 1.0, $\Lambda = 10.0$.

ϵ_0	Groove angle (deg)	\bar{W}	ϕ_0	\bar{Q}	$\bar{\mu}$	\bar{M}	λ
0.2	36	0.16276	89.6383	3.1926	34.0873	16.4180	0.5456
	18	0.16278	89.6671	3.1925	34.0836	16.4170	0.5456
0.4	36	0.07820	68.9447	4.2619	75.9983	23.2960	0.5002
	18	0.07810	68.9288	4.2610	76.0908	23.3110	0.5003
0.6	36	0.56357	47.1167	5.7690	12.2224	32.4570	0.5229
	18	0.56376	47.1058	5.7687	12.2184	32.4320	0.5231
0.8	36	2.08610	33.1357	7.5015	4.5337	64.1370	0.5684
	18	2.08770	33.1610	7.5006	4.5307	63.7990	0.5695

From Table-2 it is seen that both load capacity and stability improve for 18° grooved bearing, whereas friction variable is less. The improved load may be due to higher pressure development in the larger land area. However, it can be seen that the friction forces (coefficient of friction multiplied by load) are higher for smaller grooves. This is expected from physical point of view. The load carrying capacity and friction variable of a bearing having 36° groove angle are shown in Figure-3 for various bearing numbers and eccentricity ratios. Load capacity increases with an increase in eccentricity, as expected. The friction variable decreases as the eccentricity ratio increases. The load capacity increases with bearing number, which is a function of journal speed. This increase is sharp at higher eccentricity ratio. The coefficient of friction decreases

with an increase in journal speed. The rise in friction is particularly high at lower eccentricity ratios, as shown in Figure-3. The mass parameter \bar{M} and whirl ratio λ are used as a measure of stability. These are plotted in Figure-4. The upper portion of the curve is unstable and the lower one is stable. The bearing should be operated in the stable region. The stability increases sharply at a very high eccentricity ratio but the increase is not so higher that of the \bar{M} . The stiffness and damping co-efficient changes with the bearing numbers are shown in Figures 5 to 8. The increase is higher at higher eccentricity ratios. The coefficient of friction increases with an increase in journal speed. The variation of mass parameter, \bar{M} and the whirl ratio, λ are given in Figure-4.

**Figure-3.** Variation of load capacity and friction variable with Λ ratio for various ϵ_0 .

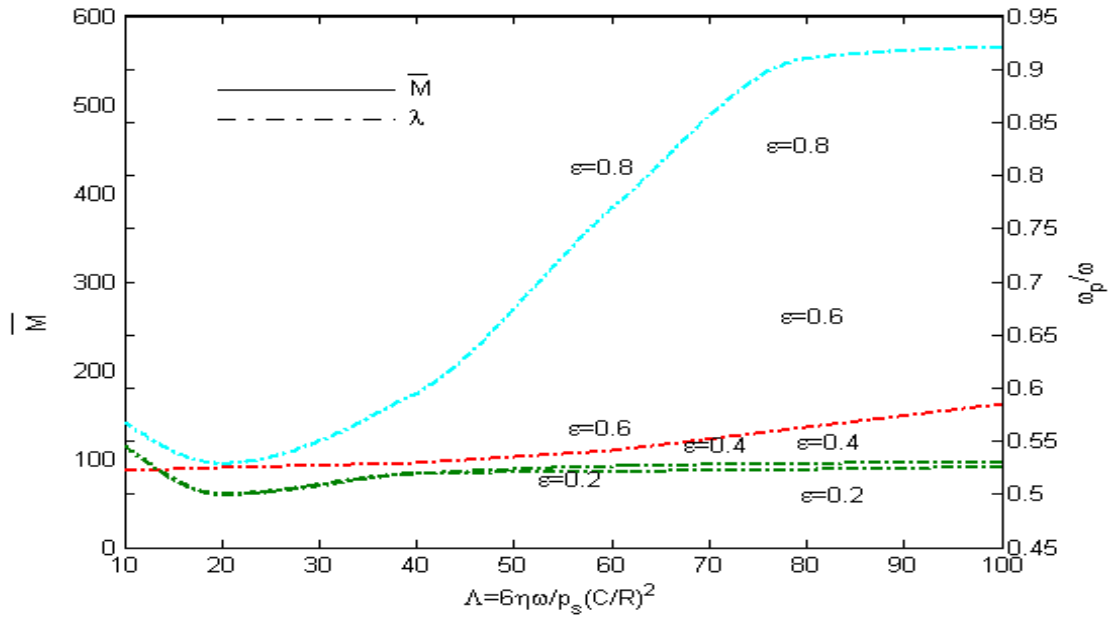


Figure-4. Variation of stability and whirl with Λ ratio for various ϵ_0 .

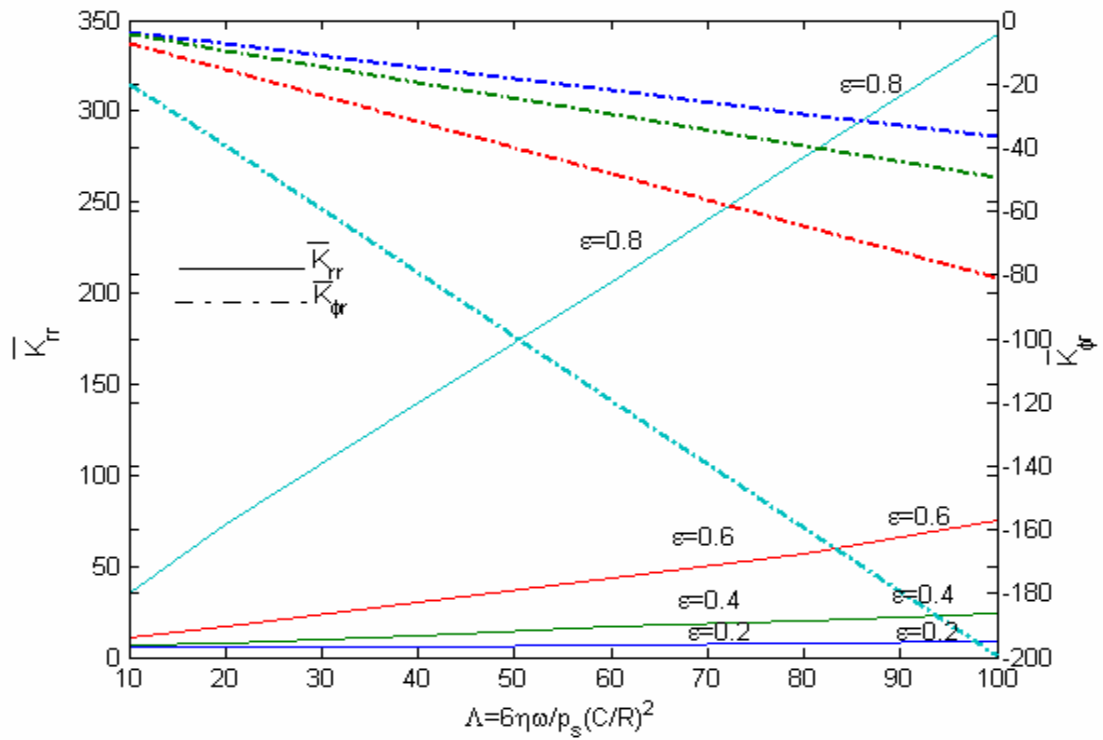


Figure-5. Variation of K_{rr} and K_{ϕ} with Λ ratio for various ϵ_0 .

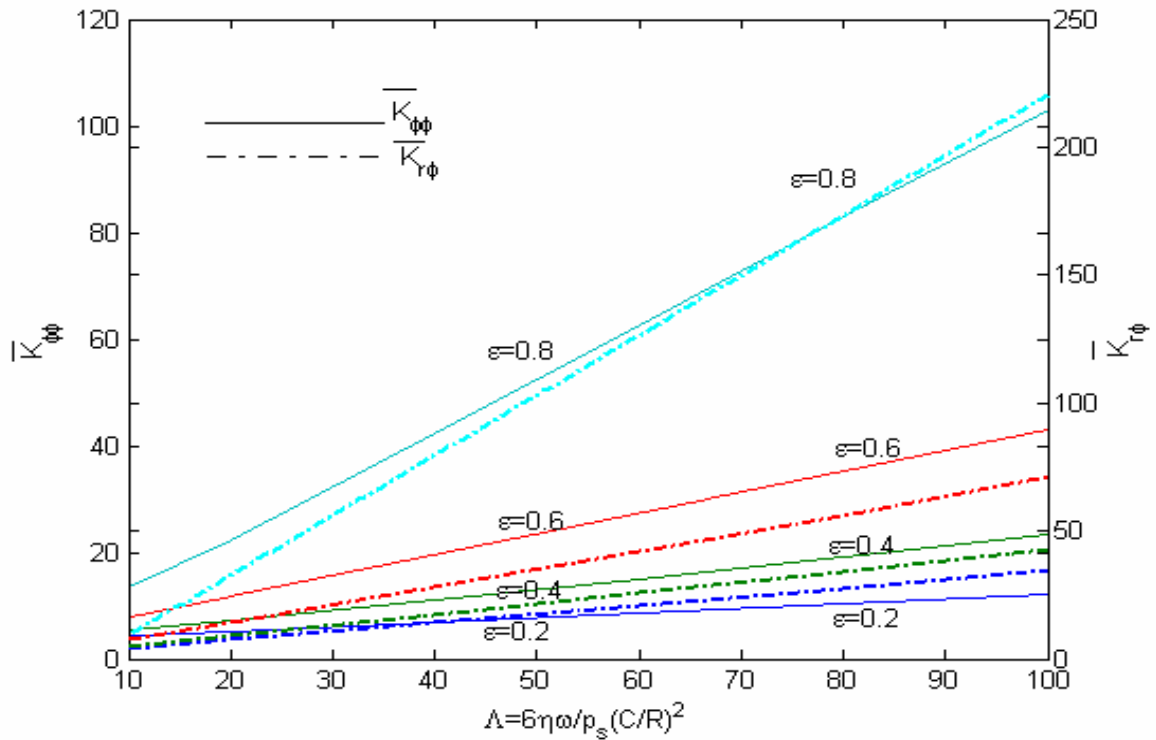


Figure-6. Variation of $K_{\phi\phi}$ and $K_{r\phi}$ with Λ ratio for various ϵ_0 .

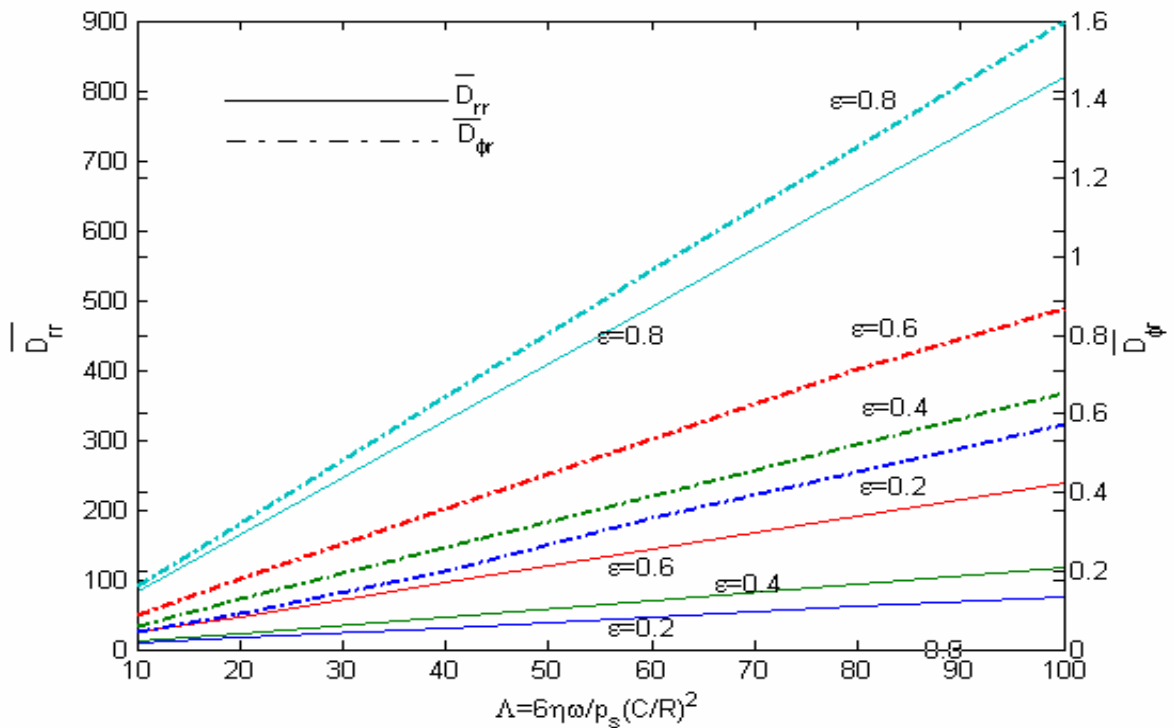


Figure-7. Variation of D_{rr} and $D_{\phi r}$ with Λ ratio for various ϵ_0 .

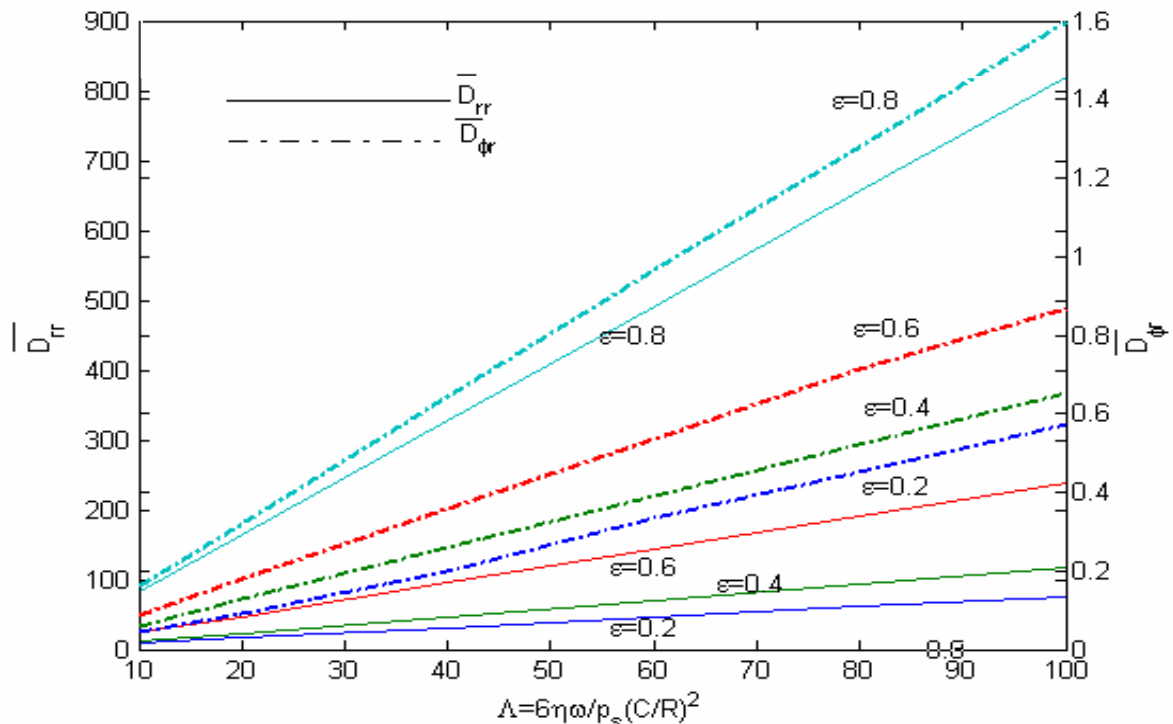


Figure-8. Variation of $D\phi\phi$ and $D\phi r$ with Λ ratio for various ϵ_0 .

4. CONCLUSIONS

The following conclusions are evident from this study:

- As expected, the load carrying capacity is more when the feeding groove chosen is smaller i.e. a bearing having smaller groove angle gives higher load capacity. This is due to high pressure in the land region. Flow rate is substantially higher.
- As the flow rate shows an increase in magnitude with eccentricity and speed it would seem to be provide removal of heat sufficiently.
- Stability improves when smaller groove angles are used. But in comparison with [9] it is much less stable.
- The stiffness and damping coefficient magnitude is higher for the bearing fed from a smaller groove angle.
- Stability increases for the bearing feeding from the top at higher eccentricity ratio. The stability also improves when smaller groove angles are used at higher speed.
- The data obtained from the above analysis can be used conveniently in the design of such bearings, as these are presented in dimensionless form.

REFERENCES

- [1] Summerfeld A. 1904. Zur hydrodynamischen Theorie de Schmiermittellburg Zeit.f. Maths.u.Phys. 40: 97-155.
- [2] Ocvirk, F.W. 1952. Short bearing approximation for full journal bearings. NACA TN 2808.
- [3] Christopherson, D.G. 1941. A new mathematical method for the solution of film lubrication problems. Proc. Instn Mech Engrs. 146: 126-135.
- [4] Raimondi, A. A. and Boyd, J.A. 1958. A solution for the finite journal bearing and its application to analysis and design, I, II and III. ASLE Trans. 1: 159-209.
- [5] Cole, J. and Hughes, C.J. 1956. Oil flow and film extent in complete journal bearing. Proc. Instn Mech Engrs. 170: 499-510.
- [6] Akers. P.E. and Flack, R.D. 1980. Journal bearing design for high speed turbo-machinery. In: Bearing Design-Historical Aspects, Present Technology and Future Problems (Ed. W.J. Anderson). Vol. 11, pp. 1-160 (ASME, New York).
- [7] F.A. Martin and C.S. Lee. 1982. Feed-pressure flow in plain journal bearings. ASLE Transactions. 26(3): 381-392.
- [8] Yoshimoto S., Anno Y., Tamura M., Kakiuchi Y. and Kimura K. 1966. Axial load capacity of water lubricated hydrodynamic conical bearings with spiral grooves. Trans. ASME, J. Tribology. 118: 893-899.
- [9] Majumder B.C., Pai. R., Hargreaves D.J. 2004. Analysis of water lubricated journal bearing with multiple axial grooves. Proc. Instn Mech Engrs. Vol. 218 Part J, Engineering Tribology. pp. 135-146.